Published in final edited form as:

Nat Biotechnol. 2014 April ; 32(4): 364–372. doi:10.1038/nbt.2858.

Development and function of human innate immune cells in a humanized mouse model

Anthony Rongvaux[a,*], **Tim Willinger**[a,*], **Jan Martinek**[c,d], **Till Strowig**[a,$], **Sofia V. Gearty**[a], **Lino L. Teichmann**[e,f], **Yasuyuki Saito**[g], **Florentina Marches**[c], **Stephanie Halene**[h], **A. Karolina Palucka**[c], **Markus G. Manz**[g,#], and **Richard A. Flavell**[a,b,#]

[a]Department of Immunobiology Yale University, New Haven CT06520, USA [b]Howard Hughes Medical Institute, Yale University, New Haven CT06520, USA [c]Baylor Institute for Immunology Research, Dallas TX75204, USA [d]Department of Biomedical Studies, Baylor University, Waco, TX 76706, USA [e]Department of Laboratory Medicine, Yale University, New Haven CT06520, USA [f]Department of Medicine III, University Hospital Bonn, 53127 Bonn, Germany [g]Division of Hematology, University Hospital Zurich, 8091 Zurich, Switzerland [h]Section of Hematology, Department of Internal Medicine and Yale Comprehensive Cancer Center, Yale University, New Haven 06520 CT, USA

Abstract

Mice repopulated with human hematopoietic cells are a powerful tool for the study of human hematopoiesis and immune function in vivo. However, existing humanized mouse models are unable to support development of human innate immune cells, including myeloid cells and NK cells. Here we describe a mouse strain, called MI(S)TRG, in which human versions of four genes encoding cytokines important for innate immune cell development are knocked in to their respective mouse loci. The human cytokines support the development and function of monocytes/macrophages and natural killer cells derived from human fetal liver or adult $CD34^+$ progenitor cells injected into the mice. Human macrophages infiltrated a human tumor xenograft in MI(S)TRG mice in a manner resembling that observed in tumors obtained from human patients. This humanized mouse model may be used to model the human immune system in scenarios of health and pathology, and may enable evaluation of therapeutic candidates in an *in vivo* setting relevant to human physiology.

Small animal models such as mice are frequently used for in vivo studies of mammalian—especially human—immune responses. However, fundamental differences in immune function exist between species[1,2] and frequently, knowledge gained from mouse studies cannot be translated to humans.

[#]Address correspondence to R.A.F. (richard.flavell@yale.edu) or M.G.M. (markus.manz@usz.ch).
[*]These authors contributed equally
[$]Present address: Helmholtz Centre for Infection Research, 38124 Braunschweig, Germany

One promising approach for studying human immune function in vivo is to use immunodeficient mice transplanted with human hematopoietic stem and progenitor cells[2,3]. However, the development and function of several human immune cell types, such as monocytes/macrophages and NK cells, is largely defective in currently available models of humanized mice[2]. More specifically, human monocytes/macrophages are present in low frequency[4,5] and while a report showed that these cells are functional[4], another report identified functional impairments and an immature phenotype of human monocytes[6]. The maturation, function and homeostasis of human NK cells are also defective in existing humanized mice[7,8]. These limitations highlight a need to develop humanized mice that model a more complete and functional human innate immune system.

The defects in human innate immune cell development in existing humanized mice are most likely due to limited reactivity of mouse cytokines with corresponding human cytokine receptors[9]. Several strategies attempting to circumvent this issue by delivering human cytokines to the mouse host have been described[10,11]; some have administered exogenous cytokines[7] or cytokine-encoding plasmids[5,12], whereas others have introduced transgenes encoding human cytokines[13-15]. However, high systemic concentrations of cytokines can result in artefactual effects such as the mobilization and exhaustion of hematopoietic stem cells[13] or supra-physiological cell frequencies.

The approach of knocking in human cytokine genes to replace their mouse counterparts has the advantage of ensuring appropriate tissue-, cell- and context-specific expression of the human cytokine[10]. Furthermore, in the scenario of homozygous human cytokine knockin mice, if the human cytokine is not fully reactive with the corresponding mouse cytokine receptor, mouse cell populations dependent on signaling from that cytokine may exhibit numerical or functional defects; these defects confer an additional competitive advantage on transplanted human cells[10]. This KI gene replacement strategy was used to ‘humanize’ several cytokine-encoding genes. For example, humanization of the gene encoding thrombopoietin (*Tpo*) resulted in enhanced maintenance of functional human hematopoietic stem cells capable of multilineage differentiation, of sustaining long-term high engraftment in the bone marrow and of serial transplantation[16]; humanization of the genes encoding interleukin-3 (*Il3*) and GM-CSF (*Csf2*) lead to the development of functional human alveolar macrophages[17]; and humanization of the *Csf1* gene, which encodes M-CSF, resulted in increased numbers of human monocytes/macrophages in multiple tissues[18]. Although each of these gene replacements improved the development and function of individual cell types (Supplementary Table 1), they did not result in a complete and robust human myelo-monocytic system in a mouse.

Modeling of the complete human monocyte and macrophage compartment is important because monocytes and macrophages play major roles in tissue homeostasis, inflammation, tumorigenesis and in the response to infectious agents[19,20]. Two general classes of macrophages have been defined on the basis of their gene expression profile, secretome composition and effector activity[21]: the classically-activated M1 subtype that displays pro-inflammatory and microbicidal activities, and the alternatively-activated M2 subtype characterized by immunoregulatory, anti-parasite and tissue repair roles. That said, this dichotomy is probably an over-simplification and a spectrum of functionally distinct

macrophage subsets likely exists. Regardless, the M1/M2 paradigm of macrophage differentiation is relevant to a number of human pathologies, including cancer[21-23]. For example, M1-like tumor-infiltrating macrophages show tumoricidal activity, while M2-like macrophages in the tumor microenvironment promote tumor growth by providing proliferative, anti-apoptotic and pro-angiogenic signals; these signals also enable cancer cell egress from primary tumors and formation of metastases[23,24]. Clinical observations indicate that myeloid cells infiltrate several types of tumors and in most cases, high densities of infiltrating macrophages correlate with poor patient prognosis[23-26].

To develop a humanized mouse model to study this and other human macrophage-related phenomena, we hypothesized that a synergy between multiple humanized cytokines would enable the full recapitulation of human myeloid development and function in the mouse. Therefore, we generated immunodeficient *Rag2*$^{-/-}$*Il2rg*$^{-/-}$ mice[27] in which the genes encoding human M-CSF[18], human IL-3 and GM-CSF[17] and human TPO[16] are knocked in to their respective mouse loci[10]; these mice are referred to as MITRG. Where indicated (MISTRG) these mice also bear a BAC-transgene encoding human SIRPα[28]. SIRP1α binds to CD47 and the resulting signal suppresses phagocytosis of CD47-expressing cells. Because human CD47 constitutively expressed on human cells binds efficiently to the mouse BAC-Tg-encoded human SIRPα, this transgene enables mouse phagocytes to 'tolerate' and not engulf engrafted human cells[28,29]. These mice are highly permissive for human hematopoiesis. In particular they harbor functional myelo-monocytic cells exhibiting subset diversity and numbers unprecedented in all previously available humanized mouse models and closely resembling those in humans. Using these mice we find that human monocytes act as a source of IL-15 trans-presentation, and support the development and function of human NK cells. Notably, we show that human myeloid cells infiltrate a human tumor grafted onto these mice; these tumor-infiltrating cells exhibit an immunosuppressive M2-like phenotype and correlate with tumor growth. By providing a more complete and functional model of the human innate immune system, MI(S)TRG mice may enable application of humanized mice to new areas of translational research.

Results

Hematopoietic engraftment in MI(S)TRG mice

Newborn MISTRG mice and their littermates MITRG (lacking the h*SIRPA* transgene) were sub-lethally irradiated and transplanted with human fetal liver-derived CD34^{+} cells, following a standard protocol[27] (see also Methods). *Rag2*$^{-/-}$*Il2rg*$^{-/-}$ mice that share the same genetic background (129xBalb/c N2) but lack all the humanized alleles, and commercially available NOD-*Scid Il2rg*$^{-/-}$ (NSG) mice served as controls. Blood engraftment (percent of hCD45^{+} cells among all CD45^{+} cells (including human and mouse CD45); Fig. 1a, b and Supplementary Fig. 1a) in NSG recipients was higher than in *Rag2*$^{-/-}$*Il2rg*$^{-/-}$ recipients, as previously reported [28,30]. The percentage of blood hCD45^{+} cells was similar in MISTRG, MITRG and in NSG, suggesting that the humanization of the four cytokine genes overcomes the need to induce phagocytic tolerance through SIRPα/CD47 cross-reactivity[28,29,31], possibly due to defects in the mouse innate response caused by the absence of mouse cytokines. Mice with at least 10% hCD45^{+} cells in the blood were selected for further

experiments (Supplementary Fig. 1b). In the bone marrow (BM), the percentages of hCD45$^+$ cells averaged approximately 90% in MI(S)TRG recipients (Fig. 1a, c and Supplementary Fig. 1c-e), and the high efficiency of engraftment in the BM was also independent of SIRPα/CD47 interaction. MISTRG mice can also be engrafted with human CD34$^+$ cells isolated from cord blood or from peripheral blood of adult donors after G-CSF mobilization (Supplementary Fig. 2).

To test the capacity of humanized cytokines to support human hematopoiesis in more competitive conditions, we transplanted human fetal CD34$^+$ cells into non-irradiated MISTRG mice. This protocol resulted in human CD45$^+$ cells in the blood and BM of all recipients (Fig. 1d, e) and, remarkably, half of the mice showed chimerism as high as the highest levels measured in recipients engrafted after X-ray pre-conditioning (compare Fig. 1e to Fig. 1b, c). These results show that the humanization of multiple cytokines creates a microenvironment in which human hematopoiesis can almost completely displace mouse hematopoiesis in the bone marrow, and obviate the need for pathology-inducing irradiation.

Functional human myeloid cells in MI(S)TRG mice

Next we assessed the capacity of MI(S)TRG mice to support human myelopoiesis. Human myeloid cells (hCD33$^+$) were present in significantly higher proportions in the blood and bone marrow of MI(S)TRG compared to *Rag2*$^{-/-}$*Il2rg*$^{-/-}$ and NSG recipients (Fig. 2a and Supplementary Fig. 3a-c). The increased proportion of myeloid cells in MI(S)TRG resulted in a blood composition resembling that of human blood, which is rich in myeloid cells and radically different from that of lymphoid-rich mouse blood[1,2] (Fig. 2b and Supplementary Fig. 3d). A similar composition was observed in the blood of MISTRG mice engrafted without irradiation (Supplementary Fig. 3e). Notably, human myeloid cells were also present in high numbers (exceeding those in NSG recipients by approximately 10-fold) in non-lymphoid tissues such as lung, liver and colon of MI(S)TRG, as shown by immunohistochemistry (hCD68$^+$ cells; Fig. 2c) and flow cytometry (hCD33$^+$; Supplementary Fig. 3f-g). Although both human monocytes (CD33^{hi}SSC^{lo}CD66$^-$) and neutrophils (CD33$^+$SSC^{hi}CD66$^+$) were present in the BM of MI(S)TRG mice (Supplementary Fig. 4a-b), the human myeloid cell populations in peripheral blood of MI(S)TRG mice were composed mostly of monocytes (Supplementary Fig. 4c); this observation suggests that terminal differentiation, egress from the BM or peripheral survival of human neutrophils is still suboptimal in this mouse environment. MISTRG mice also supported the development of human eosinophils (Siglec-8$^+$SSC^{hi}) and basophils (FcεRIα$^+$) in the bone marrow and blood (Supplementary Fig. 4d-g) and to a lesser degree in the lung (data not shown). Human dendritic cells (including conventional and plasmacytoid DCs) were also present in MISTRG mice and they underwent maturation after in vivo stimulation with lipopolysaccharide, suggesting that they are functional (Supplementary Fig. 5).

In humans, three subsets of monocytes have been phenotypically and functionally described based on differential expression of CD14 and CD16[19,32] (CD14$^+$CD16$^-$, CD14$^+$CD16$^+$ and CD14^{dim}CD16$^+$). All three subpopulations were present in the blood as well as lymphoid and non-lymphoid tissues (e.g., lung and liver) of MI(S)TRG mice (Fig. 2d, e and Supplementary Fig. 6a, b). In contrast, NSG mice harbored a lower frequency of total

myeloid cells and very few $CD14^{dim}CD16^{+}$ cells. Staining with additional markers including CD33, CD11b, CD115, CD62L and CX_3CR1 indicated that in most cases the monocyte subpopulations found in MISTRG mice closely resembled their counterparts in human peripheral blood and BM (Fig. 2f and Supplementary Fig. 7).

Next we assessed the function of human monocytes in MI(S)TRG mice. Human $CD14^{+}CD16^{-}$ and $CD14^{+}CD16^{+}$ monocytes isolated from the BM of MITRG mice produced tumor necrosis factor (TNFα) and interleukin 6 (IL-6) in response to stimulation with lipopolysaccharide (TLR4 agonist) and R848 (TLR7/8 agonist) (Fig. 3a, b). In addition, $CD14^{+}CD16^{-}$ and $CD14^{+}CD16^{+}$ cells from MITRG mice phagocytosed GFP-expressing *E. coli* in vitro; $CD14^{dim}CD16^{+}$ monocytes had limited phagocytic ability (Fig. 3c), reflecting the physiological properties of the corresponding subpopulations in human blood[32]. After injection with LPS or infection with *Listeria monocytogenes* or influenza A we detected higher amounts of human TNFα, IL-6 and interferon-β (IFNβ) in the tissues of MI(S)TRG compared to NSG mice (Fig. 3d-f). These results demonstrate that the human monocyte subsets that develop in MI(S)TRG mice are functional in vitro and in vivo.

A drawback of the high human engraftment levels and human myeloid cell function is defective development of mouse red blood cells (RBCs), particularly after irradiation, and their phagocytosis by human macrophages. As the development of human RBCs is also inefficient, human hematopoietic engraftment in MI(S)TRG promotes progressive destruction of mouse RBCs and anemia ultimately ensues; the incidence of anemia in these mice correlates with engraftment levels **[AR: OK]** higher than ∼60% $hCD45^{+}$ cells in the blood. This leaves a period of ∼2-3 weeks to perform experiments on healthy mice before the development of anemia, as detailed in the Methods section. For experiments requiring longer periods of analysis, the onset of anemia can be delayed and the lifespan of engrafted MI(S)TRG mice can be extended. One way this can be achieved is by injecting human cells into recipient mice without irradiating the recipient mice. Indeed, non-irradiated MISTRG mice with human engraftment levels of 60-80% in the blood were healthy and did not show any signs of anemia (e.g. the mice in Figure 1e). Alternatively, a lower number of human fetal liver $CD34^{+}$ donor cells can be injected; on a population basis this leads to lower engraftment levels. Lastly, adult human $CD34^{+}$ cells, which engraft less efficiently than human fetal liver $CD34^{+}$ cells, can be used. Notably, even with lower overall engraftment levels, MI(S)TRG mice retain all of their advantages over NSG mice, such as superior myelopoeisis and NK cell development.

Human NK cells in MISTRG mice

By producing cytokines, myeloid cells can support the development and differentiation of other immune cells. As such we investigated whether the improved human myeloid compartment in MISTRG mice could be a source of human cytokines, such as IL-15 trans-presented by IL-15Rα, which are essential for development of human NK cells[33]. Human IL-15 and IL-15Rα mRNA transcripts were more than 10-fold more abundant in MI(S)TRG compared to NSG liver and lung (Fig. 4a and Supplementary Fig. 8a). Next we measured the abundance of human IL-15 and IL-15Rα mRNA transcripts in purified human cell populations. Expression of human IL-15Rα mRNA was higher in human myeloid cells

(hCD33$^+$) than non-myeloid cells (hCD33$^-$) (Fig. 4b). Human CD14$^+$CD16$^+$ monocytes expressed particularly high amounts of IL-15 and IL-15Rα mRNA transcripts (Fig. 4b). Next we confirmed expression of human IL-15Rα protein on the surface of human myeloid cells from MISTRG by flow cytometry (Supplementary Fig. 8b). Although human CD14$^+$CD16$^+$ monocytes did not express significantly higher amount of surface IL-15Rα than CD14$^+$CD16$^-$ monocytes, high background staining made it difficult to accurately compare surface IL-15Rα expression between the two subsets.

Based on these findings, we analyzed the development of human immune cells dependent on IL-15 trans-presentation, such as NK cells, in MI(S)TRG mice[33,34]. Efficient development of human NK cells in existing humanized mouse models requires injection of exogenous human IL-15/IL-15Rα [7,12]; because mouse IL-15/IL15Rα is not sufficient to support human NK cells in vivo. As previously reported[7,8,12], we observed very few human NK cells (hNKp46$^+$hCD3$^-$) in engrafted NSG mice (Fig. 4c, d and Supplementary Fig. 9a, b). In contrast, human NK cells were readily detected (at 10-fold higher numbers compared to NSG mice) in multiple tissues of engrafted MISTRG mice (Fig. 4c, d and Supplementary Fig. 9a, b). With the exception of the bone marrow, MITRG mice contained fewer human NK cells than MISTRG mice, most likely due to the previously reported requirement for human SIRPα for the survival of human NK cells in the periphery[31]. The hNKp46$^+$hCD3$^-$ cells in MISTRG mice represented bona fide NK cells because like human NK cells they expressed the NK cell surface markers CD94, CD161, and killer inhibitory receptors (KIRs) (Supplementary Fig. 10a, b). Expression of the maturation marker CD16 was higher on the surface of NK cells from MISTRG compared to NSG mice, suggesting that human IL-15/IL15Rα also supports maturation of NK cells in MISTRG mice (Supplementary Fig. 10c-d).

It is not known which cell(s) are responsible for trans-presentation of IL-15 in vivo in humans; however, human myeloid cells can support human NK cell proliferation in vitro[7]. To test if trans-presentation of human IL-15 by human monocytes/macrophages underlies the improved human NK cell development in MISTRG mice, we treated MISTRG mice with liposome-encapsulated clodronate to deplete phagocytic cells. Depletion of phagocytic cells significantly reduced the number of human NK cells, but not human T cells, in MISTRG mice (Fig. 4e-f), suggesting that human monocytes/macrophages are indeed a critical source of trans-presented IL-15 in MISTRG mice. However, we cannot formally exclude other possible explanations for the enhanced human NK cell development in MISTRG mice, such as direct effects of the knocked-in human cytokines on NK cells or secondary interactions between NK cells and other human or mouse cell types.

Next we examined the function of human NK cells in MISTRG mice. NK cells defend against pathogens by killing cells that lack surface MHC class I expression[35], and by producing the IFN-γ [36]. Compared to human NK cells from NSG mice, NK cells from MISTRG mice expressed higher amounts of the lytic granule protein perforin (Fig. 5a-b) and exhibited significantly enhanced cytotoxic activity against human cells lacking MHC class I in vivo (Fig. 5c). In addition, expression of human IFNγ mRNA was more than 10-fold higher in the liver of MISTRG than NSG mice two days after Listeria infection (Fig. 5d), and more NK cells from Listeria-infected MISTRG than NSG mice produced higher amounts of human IFN-γ without ex vivo re-stimulation) (Fig. 5e-f). NK cells in MISTRG

mice also showed more degranulation (measured by plasma membrane exposure of CD107a) after Listeria infection (Fig. 5f). Overall these findings indicate that the efficient human myeloid cell development in MISTRG mice enables efficient development, differentiation, and function of human NK cells.

T and B lymphocyte function in MI(S)TRG mice

Whereas the human cytokines expressed in MISTRG were principally aimed at improving the human innate immune cell development, we also characterized adaptive immune cells (T and B lymphocytes) in MI(S)TRG mice. Human T and B cells were present in MI(S)TRG at lower frequencies than in NSG mice, due to the relative increase in myeloid cells in MI(S)TRG mice (Fig. 2b, Supplementary Fig. 11a, 12a). B cells mostly displayed an immature phenotype, as shown by the expression of the CD10, CD24 and CD38 markers, in both NSG and MISTRG recipients (Supplementary Fig. 11b-c). Likely as a consequence of this B cell immaturity[37], humoral immune responses were low in both strains of mice (Supplementary Fig. 11d). The majority of CD4 and CD8 T cells in the blood of NSG and MISTRG displayed a naive surface phenotype ($CCR7^+CD45RA^+$) (Supplementary Fig. 12b-c). Notably, human T cells in MISTRG mice were functional because like human NK cells they produced IFN-γ in response to Listeria infection (Supplementary Fig. 12d-e).

Tumor infiltration in MI(S)TRG mice

In addition to their roles in infection and inflammation, monocytes/macrophages can acquire immunosuppressive functions important for the resolution of inflammation and for tissue repair. These anti-inflammatory properties, if exhibited by tumor-infiltrating macrophages, can provide a survival advantage to evolving tumors[22,23]. We thus examined the influence of human myeloid cells on tumor development in MI(S)TRG mice. We used the human melanoma cell line Me290 as a tumor model[38]. In agreement with clinical observations showing that myeloid cells infiltrate tumors in several solid tumors[23-26], we detected more human myeloid cell infiltration in tumors in MI(S)TRG than in NSG mice, as shown by the expression of human *PTPRC* mRNA (encodes CD45) and *ITGAM* mRNA (encodes CD11b) in subcutaneously grafted Me290 tumors (Fig. 6a). Cells expressing the macrophage markers CD163 and CD14 were abundant in tumors in MISTRG mice and in tumors from human patients, but were almost undetectable in the tumors in NSG mice (Fig. 6b, c; and Supplementary Fig. 13). $CD163^+$ cells also expressed low levels of HLA-DR and high levels of CD206 (Fig. 6b, d), an immunophenotype generally associated with M2-like macrophages.

We hypothesized that M2-like macrophages infiltrating tumors in MISTRG may promote tumor growth. Supporting this hypothesis, the tumors in engrafted MI(S)TRG mice, which are heavily infiltrated by human $CD163^+$ HLA-DR^{low} $CD206^+$ macrophages, were significantly larger than tumors in NSG mice, which are not infiltrated by human macrophages; tumors in engrafted NSG mice are similar in size to tumors in non-engrafted NSG or MI(S)TRG mice (Fig. 6e, f). One way macrophages support tumor growth is by producing cytokines or enzymes that promote vascularization and immune suppression. VEGF is one such molecule[39,40], and to test whether it was involved in tumor growth in MISTRG mice, we treated the mice with the human-VEGF inhibitor Avastin™. This

treatment completely inhibited the tumor growth in engrafted MI(S)TRG mice (Fig. 6f), suggesting that engrafted cells, potentially including myeloid cells, in MI(S)TRG mice support tumor growth through a mechanism that involves VEGF activity. In aggregate these results show that MI(S)TRG mice recapitulate the role of human macrophages in tumor development and fulfill a critical need for models that enable study of the interaction between human tumors and human macrophages in vivo.

Discussion

Despite their great promise for translational research, existing humanized mouse models do not permit efficient development of human innate immune cells. The MI(S)TRG model described here overcomes this major limitation. As such, MI(S)TRG mice may uniquely enable study of fundamental questions regarding the biology of the human immune system, in vivo modeling of human diseases, and preclinical in vivo testing of new drug candidates.

The high efficiency of human hematopoietic engraftment (e.g., human cells almost completely replace mouse cells in the bone marrow) and robust development of diverse subsets of human innate immune cells in MI(S)TRG mice is due to the synergistic effect of cytokines that support successive steps and multiple lineages of human hematopoiesis, as well as to the secondary provision of additional cytokines by human cells themselves. The fact that MISTRG can be efficiently engrafted without irradiation further illustrates the advantage of the combined replacement of multiple mouse cytokine genes with their human counterparts. The absence of mouse cytokines results in defects in mouse cell populations (in particular mouse HSC and phagocytic cells) and induces a state of genetic preconditioning.

MI(S)TRG will facilitate the engraftment of hematopoietic cells derived from the peripheral blood and/or bone marrow of humans with disease. This will allow the reconstitution of a patient-derived immune system, and may permit the study of low-proliferative, primary human hematopoietic malignancies, such as myelodysplastic syndromes or myeloproliferative neoplasia, that thus far have proven difficult to efficiently engraft **[AR: OK]** immunodeficient mice[41,42].

Furthermore, a human immune system can be combined with co-transplantation of diseased tissues from the same donor; this may be relevant to autoimmune diseases and cancer. This will create a personalized model wherein the interaction of the patient's immune system with cancer cells or autoimmune target tissues can be studied in vivo. Moreover, the effect of drugs on the immune system and co-transplanted tissues can be evaluated preclinically, and treatments could be tailored to the individual patient in a personalized manner. An implication of our tumor xenograft experiments is that the outcome of anti-tumor drug treatment is markedly affected by the presence or absence of tumor-infiltrating human immune cells. Therefore, the role of non-tumoral cells, including but not limited to human myeloid cells, should be considered and carefully evaluated in screening of candidate anti-tumor drugs.

MI(S)TRG mice will also enable study of the human innate immune system in acute and chronic inflammation as well as in infectious disease. Indeed, the function of monocytes/macrophages is highly dependent on in vivo contexts that cannot be easily modeled in vitro. For example, $CD16^+$ monocytes, which develop in the MISTRG model but not in other humanized mouse models, are expanded in humans in inflammatory settings including those caused by HIV infection and atherosclerosis[43]. However, the functional significance of $CD16^+$ monocytes in these settings is unknown; MI(S)TRG mice may enable the investigation of causal relationships between $CD16^+$ monocytes and human inflammatory disease. Macrophages are also prominent in humans infected with bacteria including *Mycobacterium tuberculosis*[44]. Further improvements of the adaptive immune system function in MI(S)TRG mice (see below) should enable study of the interaction between human macrophages, CD4 T cells, and *Mycobacterium tuberculosis* in vivo. Standard non-humanized mice do not represent this complex human disease faithfully. Other fundamental questions that may be answered using the MI(S)TRG model include the ontogenic origin of tissue macrophages vs. monocyte-derived macrophages[45], the trafficking of these cells in response to inflammation or infection, and the mechanisms of differentiation and effector function of M1 vs. M2 macrophages[46].

Finally, MISTRG mice will allow study of the role of human NK cells in vivo, for example in the context of cancer and viral infections[47].

Although MISTRG mice represent a marked improvement over existing humanized mouse models, they also have two drawbacks. First, as mentioned earlier development and survival of both mouse and human RBCs is suboptimal in MI(S)TRG mice. This problem will need to be addressed in the future by genetic strategies to either protect mouse RBCs from phagocytosis by human cells, or to support the development and survival of human RBCs.

The other limitation of MI(S)TRG mice, similarly to other models, is their relatively weak adaptive immune responses, with low cytotoxic and humoral immune responses, particularly a low frequency of somatic mutation and class-switching in B cells. Adaptive immunity might be improved by a number of approaches, including expression of human MHC elements in mice or use of the bone marrow-liver-thymus (BLT) approach where human fetal tissues are transplanted along with human $CD34^+$ cells[48,49]. The BLT approach results in more robust adaptive immune responses because T cells develop and are selected in a human thymic tissue. A non-mutually exclusive approach would be humanizing additional cytokine genes in recipient mice. By combining multiple strategies, humanized mouse models may fully recapitulate functional human innate and adaptive immune responses. Such mouse models may enable an even wider variety of basic and pre-clinical research applications.

methods

Mice

The knockin replacement (from ATG to STOP codon) of individual loci (encoding TPO, IL-3/GM-CSF or M-CSF) in the *Rag2*$^{-/-}$ *Il2rg*$^{-/-}$ 129xBalb/c (N2) genetic background was performed using Velocigene Technology in collaboration with Regeneron Pharmaceuticals,

as reported previously[16-18]. Human SIRPα expression was achieved by BAC-transgenesis in the same genetic background[28]. We intercrossed these strains by conventional breeding to obtain MITRG (M-CSF$^{h/h}$ IL-3/GM-CSF$^{h/h}$ TPO$^{h/h}$ *Rag2*$^{-/-}$ *Il2rg*$^{-/-}$) and MISTRG (M-CSF$^{h/h}$ IL-3/GM-CSF$^{h/h}$ hSIRPA^{tg} TPO$^{h/h}$ *Rag2*$^{-/-}$ *Il2rg*$^{-/-}$) mice. We maintained them under specific pathogen free conditions with continuous treatment with enrofloxacin in the drinking water (Baytril, 0.27 mg/ml). MITRG and MISTRG are viable for 1 year or more and have normal fertility at least until 8 months old. NOD *Scid Il2rg*$^{-/-}$(NSG) mice were obtained from The Jackson Laboratory.

MITRG and MISTRG mice have been deposited at The Jackson Laboratory. [AU: these stock numbers do not retrieve any mice on the JAX website—if the numbers will not be functional by the time this paper is published please delete them from this manuscript] **[AR: we don't have any information on when these strains will appear on the JAX website. The transfer of the mice is currently in progress]**

Human progenitor cell isolation and injection

Recipient mice were engrafted with human hematopoietic stem and progenitor cells as previously described[16-18,27,28]. Briefly, human fetal liver samples were cut in small fragments, treated for 45 min at 37°C with Collagenase D (Roche, 100 ng/mL) and a cell suspension was prepared. Human CD34$^+$ cells were purified from fetal liver samples or from cord blood by density gradient centrifugation (Lymphocyte Separation Medium, MP Biomedicals) followed by positive immunomagnetic selection with anti-human CD34 microbeads (Miltenyi Biotec). Cells were frozen in FBS containing 10% DMSO and kept in liquid nitrogen. G-CSF-mobilized adult CD34$^+$ cells were obtained from the Department of Laboratory Medicine, Yale University or the Division of Hematology, University Hospital Zurich. All human studies were approved by the Yale University Human Investigation Committee or the Cantonal ethics committee of Zurich, Switzerland.

Newborn mice (within first 2 days of life) were sublethally irradiated (X-ray irradiation with X-RAD 320 irradiator, PXi; *Rag2*$^{-/-}$*Il2rg*$^{-/-}$, 2 × 180 cGy 4 h apart; NSG, 1 x 100 cGy; MI(S)TRG, 1 × 150 cGy) and 100,000 CD34$^+$ cells in 20 μL of PBS were injected into the liver with a 22-gauge needle (Hamilton Company). Unless otherwise specified, all mice were transplanted with CD34$^+$ cells isolated from fetal liver. In specific experiments (Fig. 1d, e), 200,000-300,000 FL-CD34$^+$ cells were injected into non-irradiated MISTRG newborn recipients. The mice were bled 7-9 weeks later and the percentage of human CD45$^+$ cells was measured by flow cytometry. Mice in which human CD45$^+$ cells represented at least 5% (*Rag2*$^{-/-}$*Il2rg*$^{-/-}$) or 10% (NSG, MITRG and MISTRG) of the total (mouse and human combined) CD45$^+$ populations were selected for further experimentation. The mice were sacrificed or used for experiments 9-12 weeks after transplantation.

The post-engraftment lifespan is ∼10-12 weeks (for MISTRG) and ∼12-16 weeks (for MITRG) when the mice transplanted with 100,000 FL-CD34+ cells after sublethal irradiation (150 cGy). The first clinical signs of anemia directly correlate with high engraftment levels, and they generally appear when engraftment levels reach ∼60% hCD45$^+$ cells in peripheral blood. Adult CD34$^+$ cells are less potent than fetal CD34$^+$ cells in that human engraftment levels do not exceed 20-30% in the peripheral blood of mice injected

with adult $CD34^+$ cells. As a consequence, mice remained alive and healthy for up to 22 weeks after engraftment with adult $CD34^+$ cells. Irradiation also contributes to anemia, as mice engrafted without irradiation remained healthy for up to 12 weeks [AU: for how long?] even with 60-80% $hCD45^+$ cells in the blood.

Mice (both males and females) of comparable engraftment levels (percentage of $hCD45^+$ cells in the blood and relative lineage composition) that were engrafted with cells from the same donor(s) were separated randomly into the experimental groups. The results presented are combined from at least 2 independent experiments, with a total of 6-12 mice/ experimental group; each independent experiment was performed with mice transplanted with $CD34^+$ cells from different donors.

As MITRG and MISTRG mice are similar in many aspects, for some experiments we used both MITRG and MISTRG mice (indicated as “MI(S)TRG”), engrafted with matched fetal liver samples and with comparable engraftment levels.

All animal experimentations were performed in compliance with Yale Institutional Animal Care and Use Committee protocols.

Immunophenotypic analysis of human cell populations

To prepare white blood cells from engrafted mice, heparinized blood was treated twice with ACK lysis buffer to eliminate RBCs. For the spleen and bone marrow, single cell suspensions (flushed from the femur and tibia in the BM) were treated with ACK lysis buffer. Liver and lung leukocytes were isolated by mechanically dissociating and digesting tissues with 100 U/ml collagenase IV and 0.02 mg/ml DNase I (Sigma) for 1h at 37°C, followed by density gradient centrifugation.

For FACS analysis, antibodies against the following antigens were used:

Mouse antigens: CD45 (clone 30-F11)

Human antigens: CD1c (BDCA1, clone L161), CD3 (UCHT1), CD4 (OKT4), CD8 (HIT8a) CD10 (HI10a), CD11b (ICRF44), CD11c (B-ly6, BD Biosciences), CD14 (M5E2), CD16 (3G8), CD19 (HIB19), CD20 (2H7), CD24 (ML5), CD33 (WM53), CD38 (HIT2), CD45 (HI30), CD45RA (HI100), CD62L (DREG-56), CD66 (ASL-32), CD94 (DX22), CD107a (H4A3), CD115 (9-4D2-1E4), CD123 (6H6), CD141 (BDCA3, M80), CD161 (HP-3G10), CD303 (BDCA2, 201A), NKp46 (9E2), IL-15Rα (JM7A4), CCR7 (150503, R&D Systems), CX3CR1 (2A9-1), FcεRIα (AER-37), HLA-A,B,C (W6/32), HLA-DR (L243), IFN-γ (B27) KIR2DL1/S1 (HP-MA4), KIR2DL2/L3 (DX27), KIR3DL1 (DX9), perforin (dG9), Siglec-8 (7C9).

Human lineage cocktail: CD3, CD15, CD19, CD56, NKp46—All antibodies were obtained from Biolegend, unless otherwise specified. **[AU: please specify source for each antibody]**. Data were acquired with FACSDiva on a LSRII flow cytometer (BD Biosciences) and analyzed with FlowJo software.

For histological analysis, spleen, lung, liver and colon tissues were fixed overnight in IHC zinc fixative (BD Biosciences) or 4% paraformaldehyde and embedded in paraffin. Sections were stained with hematoxylin and eosin, or with anti-human CD68 (clone PGM1) followed by a HRP-conjugated secondary antibody and revealed with the peroxidase substrate 3, 3′-diaminobenzidine.

Phagocytosis assay in vitro

E. Coli expressing GFP were grown in LB medium overnight at 37°C to an OD600 of 1.5-1.8, at which point the bacteria were diluted and grown for 1-2 hours to an OD600 of approximately 1.0. The *E. Coli* were washed three times with PBS and incubated with WBCs from MITRG mice for 4 hours at 37°C in a volume of 200μl with about 2×10^8 *E. Coli* per 1×10^7 WBCs. After the incubation, the cells were washed with PBS and analyzed by flow cytometry.

TLR stimulation in vitro and infection in vivo

Human monocyte subsets were isolated from the BM of engrafted mice. Briefly, BM cells were recovered and pooled from the hind legs and the spine of six mice. Human $CD33^+$ cells were enriched by magnetic isolation (EasySep CD33 selection kit, StemCell Technologies). $CD14^+CD16^-$ and $CD14^+CD16^+$ subsets were purified on a FACSAria cell sorter (BD Biosciences). 100,000 cells in 200 μl media were cultivated overnight in the presence of the TLR4 ligand LPS (*E. Coli* 0111:B4, Sigma-Aldrich, 100 ng/ml) or the TLR7/8 ligand R848 (Invivogen, 10 μg/ml).

For in vivo stimulation, 35 μg of LPS (*E. Coli* 0111:B4, Sigma-Aldrich) in 100 μl PBS were injected intra-peritoneally and the serum was collected 90 minutes later. For dendritic cell analysis, 10 μg of LPS was injected intra-peritoneally and the mice were sacrificed 6h later.

Mice were infected with 3×10^3 colony-forming units (CFU) of Listeria monocytogenes (strain 10403S) by intravenous injection. 48 hours after infection, sera and tissues were harvested for ELISA and qPCR, respectively. Cytokine concentrations (human TNFα, IL-6 and IL-1β) in mouse serum and in culture supernatants were measured using ELISA MAX Standard kits (Biolegend), following the manufacturer's instructions. Liver lymphocytes from uninfected or infected mice were incubated at 37C° in 5% CO_2 for 4 hours in medium containing monensin (GolgiStop, BD Biosciences) and anti-human CD107a. Cells were then stained for surface antigens (mCD45, hCD45, hNKp46 and hCD3), permeabilized using Cytofix/Cytoperm kit (BD Biosciences), and stained for intracellular human IFN-γ.

Mice were infected intranasally with 2×10^4 PFU of influenza A /PR8 (H1N1) virus, and lungs were harvested on day 3 postinfection for qPCR analysis.

Depletion of phagocytic cells in vivo

Phagocytic cells were depleted by intravenous retro-orbital injection of 100 μl of clodronate-loaded liposomes[50]. Clodronate-liposomes were injected 3 times daily and human NK cells in mouse liver were analyzed 24h after the last injection.

Quantitative RT-PCR

Total RNA was extracted from tissues or purified cells with TRIzol reagent (Invitrogen) according to the manufacturer's instructions and used for cDNA synthesis with the SuperScript First-Strand Synthesis System (Invitrogen). Quantitative RT-PCR was performed on a 7500 Fast Real-Time PCR system with primer-probe sets **[AU: please supply primer sequences or catalog numbers]** purchased from ABI (h*IFNB1*, Hs01077958_s1; h*IL15*, Hs01003716_m1; h*IL15RA*, Hs00542604_m1; h*PTPRC*, Hs04189704_m1; h*ITGAM*, Hs00355885_m1). Expression values were calculated using the comparative threshold cycle method and normalized to mouse *Hprt* (Mm00446968_m1) or human *HPRT* (Hs99999909_m1), as indicated.

In vivo NK cell cytotoxicity assays

Human NK cell cytotoxicity in vivo was determined following a previously reported protocol[8]. LCL721.221 (HLA class I negative) and LCL721.45 (HLA class I positive) cells were mixed in a 1:1 ratio, labeled with CellTrace Violet (Invitrogen) and injected intravenously (1×10^7 cells/mouse) into engrafted NSG or MISTRG mice. Mice were sacrificed 12 hours later and a single cell suspension of the spleen was prepared and analyzed by flow cytometry. The proportions of HLA class I-positive and HLA class I-negative cells among Violet-labeled cells were measured and specific lysis was calculated as (MHC class I positive − MHC class I negative) × 100 / MHC class I positive.

Immunization

Ovalbumin (Sigma-Aldrich, 100 μg/mouse) was emulsified in Complete Freund's adjuvant (Difco, primary immunization) or in Incomplete Freund's adjuvant (secondary immunization 2 weeks later). The emulsion was injected intra-peritoneally. The mice were bled before the first immunization (pre-immune serum) and 1 week after the second immunization. The presence of ovalbumin-specific human IgM in the serum was measured by ELISA, using a biotinylated anti-IgM antibody (BD Biosciences) followed by horseradish peroxidase-conjugated streptavidin (Vector Laboratories).

Tumorigenesis

The human melanoma cell line Me290[38] (kindly provided by Dr. Pedro Romero, Lausanne, Switzerland), which was mycoplasma-free (assessed by MycoAlert assay, Lonza), was grown to ∼90% confluency in the presence of Plasmocin Prophylactic (InvivoGen) and the cells (∼7 million cells per mouse) were injected subcutaneously under anesthesia in the flank of the mouse. For some experiments, the mice were treated every other day, starting on the day of tumor implantation, with the human VEGF-specific antibody Avastin™ (Roche; 100 μg intraveinously). The size of the tumors was measured, in a blinded manner when possible, 11 days later and the volume calculated using the following formula: Volume = 0.5 * Length^2 * Width.

Human tumor samples were obtained, with informed consent from the donors, from the Baylor University Medical Center Tissue Bank with approval from the Institutional Review Board.

Patient and mouse tissues were frozen in Optimum Cutting Temperature (OCT, Sakura Finetek). Cryosections (7 μm) were consecutively treated with Triton-100× 0.1% for 15 min, Hyaluronidase 0.03% for 15 min, Background Buster (Innovex bioscience) for 15 min, Fc Receptor Block (Innovex bioscience) for 15 min and Background Buster for an additional 15 min. The sections were then stained with primary antibodies, diluted in PBS supplemented with 5% BSA and 0.01% Saponin for 1h at room temperature, washed and stained with the secondary antibodies at room temperature for 40 minutes. Nuclei were stained with 4′,6-diamidino-2-phenylindole (1ug/mL) for 2 min.

Primary antibodies: human CD14 (1:200, UCHM1, AbD Serotec); human CD163 (1:200, EDHu-1, AbD Serotec); human CD206 (1:100, 15-2, AbD Serotec); human HLA-DR (1:100, LN3, Biolegend). For CD163/CD206 combined staining, both antibodies were labeled with Alexa Fluor 488 or 568 Antibody Labeling Kit (Molecular Probes) prior tissue staining.

Secondary antibodies: goat anti-rat Alexa Fluor 568; goat anti-mouse Alexa Fluor 488; goat anti-mouse Alexa Fluor 588 or goat anti-mouse Alexa Fluor 647 (1:700, Molecular Probes).

Immunofluorescence imaging was performed on an Eclipse Ti inverted microscope system (Nikon Instruments Inc.) operated via NIS-Element Ar software (Nikon Instruments Inc).

For quantification of the density of $CD163^+$ cell infiltration, tumors from 3 different melanoma patients, 3 NSG and 3 MISTRG were selected (without blinding). From each tumor, 3 cryosections were stained for human CD163. From each stained section 3 representative pictures were acquired, totaling 27 representative pictures from each group (patients, MISTRG and NSG). For each picture, $CD163^+$ cells were counted using the NIS-Element Ar software (Niko Instruments Inc.). Each picture was analyzed using the “split channels + overlay” display and by zooming simultaneously on each separate channel and on the overlay.

Statistical analysis

Statistical analysis was performed with the GraphPad Prism 6 software, using one-way ANOVA followed by Tukey post hoc test, two-tailed unpaired Student's *t*-test or repeated measure ANOVA. Similar standard deviations were determined within each of those tests. The size of the groups was determined based on the results of preliminary experiments, in order to achieve statistical significance, but without specific statistical analysis to determine pre-specified group size.

Supplementary Material

Refer to Web version on PubMed Central for supplementary material.

Acknowledgments

We thank our colleagues G. Yancopoulos, D. Valenzuela, A. Murphy and W. Auerbach at Regeneron Pharmaceuticals who generated, in collaboration with our groups, the individual knockin alleles combined in MISTRG. We thank J. Alderman for managerial support; AM. Franco, P. Ranney, C. Weibel, S. Patel and M. Santhanakrishnan for technical assistance; and G. Lyon for cell sorting; and C. Lieber for manuscript submission.

This work was supported by the Bill and Melinda Gates Foundation and NIH CA156689 (to R.A.F and M.G.M.); the University of Zurich Clinical Research Program (to M.G.M); the Juvenile Diabetes Research Foundation and the Connecticut Stem Cell Research Grants Program (to R.A.F.). R.A.F. is an Investigator of the Howard Hughes Medical Institute.

References

1. Mestas, J.; Hughes, CC. Journal of immunology. Vol. 172. Baltimore, Md.: 2004. Of mice and not men: differences between mouse and human immunology; p. 2731-2738.1950
2. Rongvaux A, et al. Human hemato-lymphoid system mice: current use and future potential for medicine. Annual review of immunology. 2013; 31:635–674.10.1146/annurev-immunol-032712-095921
3. Shultz LD, Brehm MA, Garcia-Martinez JV, Greiner DL. Humanized mice for immune system investigation: progress promise and challenges. Nature reviews Immunology. 2012; 12:786–798.10.1038/nri3311
4. Tanaka, S., et al. Journal of immunology. Baltimore, Md.: 2012. Development of Mature and Functional Human Myeloid Subsets in Hematopoietic Stem Cell-Engrafted NOD/SCID/IL2rgammaKO Mice. 1950
5. Li, Y., et al. Journal of immunology. Vol. 191. Baltimore, Md: 2013. Induction of Functional Human Macrophages from Bone Marrow Promonocytes by M-CSF in Humanized Mice; p. 3192-3199.1950
6. Gille C, et al. Monocytes derived from humanized neonatal NOD/SCID/IL2Rgamma(null) mice are phenotypically immature and exhibit functional impairments. Human immunology. 2012; 73:346–354.10.1016/j.humimm.2012.01.006 [PubMed: 22330087]
7. Huntington ND, et al. IL-15 trans-presentation promotes human NK cell development and differentiation in vivo. The Journal of experimental medicine. 2009; 206:25–34.10.1084/jem.20082013 [PubMed: 19103877]
8. Strowig T, et al. Human NK cells of mice with reconstituted human immune system components require preactivation to acquire functional competence. Blood. 2010; 116:4158–4167.10.1182/blood-2010-02-270678 [PubMed: 20671122]
9. Manz MG. Human-hemato-lymphoid-system mice: opportunities and challenges. Immunity. 2007; 26:537–541.10.1016/j.immuni.2007.05.001 [PubMed: 17521579]
10. Willinger T, Rongvaux A, Strowig T, Manz MG, Flavell RA. Improving human hemato-lymphoid-system mice by cytokine knock-in gene replacement. Trends in immunology. 2011; 32:321–327.10.1016/j.it.2011.04.005 [PubMed: 21697012]
11. Drake AC, Chen Q, Chen J. Engineering humanized mice for improved hematopoietic reconstitution. Cellular & molecular immunology. 2012; 9:215–224.10.1038/cmi.2012.6 [PubMed: 22425741]
12. Chen Q, Khoury M, Chen J. Expression of human cytokines dramatically improves reconstitution of specific human-blood lineage cells in humanized mice. Proceedings of the National Academy of Sciences of the United States of America. 2009; 106:21783–21788.10.1073/pnas.0912274106 [PubMed: 19966223]
13. Nicolini FE, Cashman JD, Hogge DE, Humphries RK, Eaves CJ. NOD/SCID mice engineered to express human IL-3, GM-CSF and Steel factor constitutively mobilize engrafted human progenitors and compromise human stem cell regeneration. Leukemia : official journal of the Leukemia Society of America, Leukemia Research Fund, U K. 2004; 18:341–347.10.1038/sj.leu.2403222
14. Brehm MA, et al. Engraftment of human HSCs in nonirradiated newborn NOD-scid IL2rgamma null mice is enhanced by transgenic expression of membrane-bound human SCF. Blood. 2012; 119:2778–2788.10.1182/blood-2011-05-353243 [PubMed: 22246028]
15. Ito, R., et al. Journal of immunology. Vol. 191. Baltimore, Md: 2013. Establishment of a human allergy model using human IL-3/GM-CSF-transgenic NOG mice; p. 2890-2899.1950
16. Rongvaux A, et al. Human thrombopoietin knockin mice efficiently support human hematopoiesis in vivo. Proceedings of the National Academy of Sciences of the United States of America. 2011; 108:2378–2383.10.1073/pnas.1019524108 [PubMed: 21262827]

17. Willinger T, et al. Human IL-3/GM-CSF knock-in mice support human alveolar macrophage development and human immune responses in the lung. Proceedings of the National Academy of Sciences of the United States of America. 2011; 108:2390–2395.10.1073/pnas.1019682108 [PubMed: 21262803]
18. Rathinam C, et al. Efficient differentiation and function of human macrophages in humanized CSF-1 mice. Blood. 2011; 118:3119–3128.10.1182/blood-2010-12-326926 [PubMed: 21791433]
19. Auffray C, Sieweke MH, Geissmann F. Blood monocytes: development, heterogeneity, and relationship with dendritic cells. Annual review of immunology. 2009; 27:669–692.10.1146/annurev.immunol.021908.132557
20. Chow A, Brown BD, Merad M. Studying the mononuclear phagocyte system in the molecular age. Nature reviews Immunology. 2011; 11:788–798.10.1038/nri3087
21. Sica A, Mantovani A. Macrophage plasticity and polarization: in vivo veritas. The Journal of clinical investigation. 2012; 122:787–795.10.1172/jci59643 [PubMed: 22378047]
22. Allavena P, Mantovani A. Immunology in the clinic review series; focus on cancer: tumour-associated macrophages: undisputed stars of the inflammatory tumour microenvironment. Clinical and experimental immunology. 2012; 167:195–205.10.1111/j.1365-2249.2011.04515.x [PubMed: 22235995]
23. Qian BZ, Pollard JW. Macrophage diversity enhances tumor progression and metastasis. Cell. 2010; 141:39–51.10.1016/j.cell.2010.03.014 [PubMed: 20371344]
24. Coussens, LM.; Zitvogel, L.; Palucka, AK. Science. Vol. 339. New York, N.Y: 2013. Neutralizing tumor-promoting chronic inflammation: a magic bullet?; p. 286-291.
25. Nelson CM, Bissell MJ. Of extracellular matrix, scaffolds, and signaling: tissue architecture regulates development, homeostasis, and cancer. Annual review of cell and developmental biology. 2006; 22:287–309.10.1146/annurev.cellbio.22.010305.104315
26. Bingle L, Brown NJ, Lewis CE. The role of tumour-associated macrophages in tumour progression: implications for new anticancer therapies. The Journal of pathology. 2002; 196:254–265.10.1002/path.1027 [PubMed: 11857487]
27. Traggiai, E., et al. Science. Vol. 304. New York, N.Y: 2004. Development of a human adaptive immune system in cord blood cell-transplanted mice; p. 104-107.
28. Strowig T, et al. Transgenic expression of human signal regulatory protein alpha in Rag2-/-gamma(c)-/- mice improves engraftment of human hematopoietic cells in humanized mice. Proceedings of the National Academy of Sciences of the United States of America. 2011; 108:13218–13223.10.1073/pnas.1109769108 [PubMed: 21788509]
29. Takenaka K, et al. Polymorphism in Sirpa modulates engraftment of human hematopoietic stem cells. Nature immunology. 2007; 8:1313–1323.10.1038/ni1527 [PubMed: 17982459]
30. Brehm, MA., et al. Clinical immunology. Vol. 135. Orlando, Fla: 2010. Parameters for establishing humanized mouse models to study human immunity: analysis of human hematopoietic stem cell engraftment in three immunodeficient strains of mice bearing the IL2rgamma(null) mutation; p. 84-98.
31. Legrand N, et al. Functional CD47/signal regulatory protein alpha (SIRP(alpha)) interaction is required for optimal human T- and natural killer- (NK) cell homeostasis in vivo. Proceedings of the National Academy of Sciences of the United States of America. 2011; 108:13224–13229.10.1073/pnas.1101398108 [PubMed: 21788504]
32. Cros J, et al. Human CD14dim monocytes patrol and sense nucleic acids and viruses via TLR7 and TLR8 receptors. Immunity. 2010; 33:375–386.10.1016/j.immuni.2010.08.012 [PubMed: 20832340]
33. Ma A, Koka R, Burkett P. Diverse functions of IL-2, IL-15, and IL-7 in lymphoid homeostasis. Annual review of immunology. 2006; 24:657–679.10.1146/annurev.immunol.24.021605.090727
34. Soderquest K, et al. Monocytes control natural killer cell differentiation to effector phenotypes. Blood. 2011; 117:4511–4518.10.1182/blood-2010-10-312264 [PubMed: 21389319]
35. Raulet DH. Missing self recognition and self tolerance of natural killer (NK) cells. Seminars in immunology. 2006; 18:145–150.10.1016/j.smim.2006.03.003 [PubMed: 16740393]
36. Vivier E, Tomasello E, Baratin M, Walzer T, Ugolini S. Functions of natural killer cells. Nature immunology. 2008; 9:503–510.10.1038/ni1582 [PubMed: 18425107]

37. Lang, J., et al. Journal of immunology. Vol. 190. Baltimore, Md: 2013. Studies of lymphocyte reconstitution in a humanized mouse model reveal a requirement of T cells for human B cell maturation; p. 2090-2101.1950
38. Valmori, D., et al. Journal of immunology. Vol. 160. Baltimore, Md.: 1998. Enhanced generation of specific tumor-reactive CTL in vitro by selected Melan-A/MART-1 immunodominant peptide analogues; p. 1750-1758.1950
39. Kandalaft LE, Motz GT, Busch J, Coukos G. Angiogenesis and the tumor vasculature as antitumor immune modulators: the role of vascular endothelial growth factor and endothelin. Current topics in microbiology and immunology. 2011; 344:129–148.10.1007/82_2010_95 [PubMed: 20680802]
40. Motz GT, Coukos G. Deciphering and reversing tumor immune suppression. Immunity. 2013; 39:61–73.10.1016/j.immuni.2013.07.005 [PubMed: 23890064]
41. Thanopoulou E, et al. Engraftment of NOD/SCID-beta2 microglobulin null mice with multilineage neoplastic cells from patients with myelodysplastic syndrome. Blood. 2004; 103:4285–4293.10.1182/blood-2003-09-3192 [PubMed: 14962905]
42. Wang X, et al. Spleens of myelofibrosis patients contain malignant hematopoietic stem cells. The Journal of clinical investigation. 2012; 122:3888–3899.10.1172/jci64397 [PubMed: 23023702]
43. Wong KL, et al. The three human monocyte subsets: implications for health and disease. Immunologic research. 2012; 53:41–57.10.1007/s12026-012-8297-3 [PubMed: 22430559]
44. Ramakrishnan L. Revisiting the role of the granuloma in tuberculosis. Nature reviews Immunology. 2012; 12:352–366.10.1038/nri3211
45. Schulz, C., et al. Science. Vol. 336. New York, N.Y: 2012. A lineage of myeloid cells independent of Myb and hematopoietic stem cells; p. 86-90.
46. Martinez FO, et al. Genetic programs expressed in resting and IL-4 alternatively activated mouse and human macrophages: similarities and differences. Blood. 2013; 121:e57–69.10.1182/blood-2012-06-436212 [PubMed: 23293084]
47. Jost S, Altfeld M. Control of human viral infections by natural killer cells. Annual review of immunology. 2013; 31:163–194.10.1146/annurev-immunol-032712-100001
48. Lan P, Tonomura N, Shimizu A, Wang S, Yang YG. Reconstitution of a functional human immune system in immunodeficient mice through combined human fetal thymus/liver and CD34+ cell transplantation. Blood. 2006; 108:487–492.10.1182/blood-2005-11-4388 [PubMed: 16410443]
49. Melkus MW, et al. Humanized mice mount specific adaptive and innate immune responses to EBV and TSST-1. Nature medicine. 2006; 12:1316–1322.10.1038/nm1431
50. Van Rooijen N, Sanders A. Liposome mediated depletion of macrophages: mechanism of action, preparation of liposomes and applications. Journal of immunological methods. 1994; 174:83–93. [PubMed: 8083541]

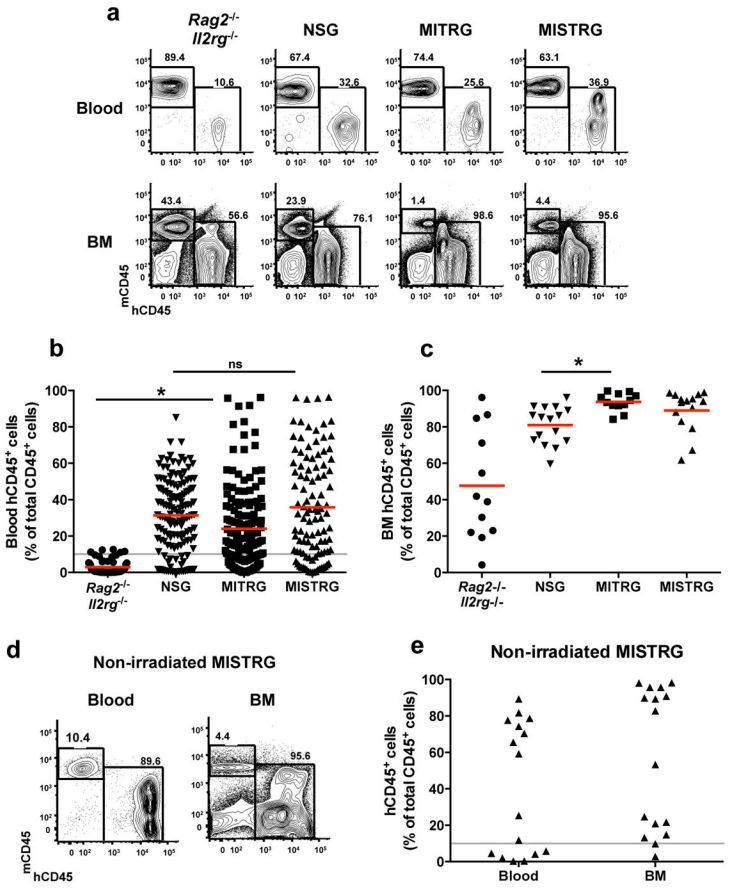

Fig. 1. Efficient engraftment of human hematopoietic cells in MI(S)TRG mice

X-ray pre-conditioned newborn mice of the indicated strains were engrafted by intra-hepatic injection of 100,000 human fetal liver CD34$^+$ cells. Human engraftment (the percentage of hCD45$^+$ cells among all (mouse and human) CD45$^+$ cells) was measured in the blood 7-9 weeks later, and in the BM 10-12 weeks later. **a**, Representative flow cytometry analysis of the frequency of mouse and human CD45$^+$ cells in the blood and BM of the indicated recipient mice. Numbers next to gated areas indicate percentages among total CD45$^+$ cells. **b**, Blood engraftment from 19 independent experiments. In each experiment, a single fetal liver CD34$^+$ cell sample was split and injected into mice of the respective strains. Each symbol represents an individual mouse and the red bars indicate mean values (n=56-155; ns, not significant; * $p<0.05$ Tukey test, see Supplementary Fig. 2a for a complete statistical analysis). The gray horizontal line indicates 10% hCD45$^+$ cells. **c**, Engraftment in the BM of a representative subset of mice (Supplementary Fig. 2c) from panel **b** (n=12-16; * $p<0.05$ Tukey test; see also Supplementary Fig. 2d-e). **d**, Representative flow cytometry analysis of hCD45$^+$ cell engraftment in the blood and BM 3 months after intra-hepatic injection of 200,000 fetal liver CD34$^+$ cells into non-irradiated newborn MISTRG mice. **e**, Human CD45$^+$ cell engraftment levels in the blood and BM of MISTRG mice transplanted as in **d** (n=16).

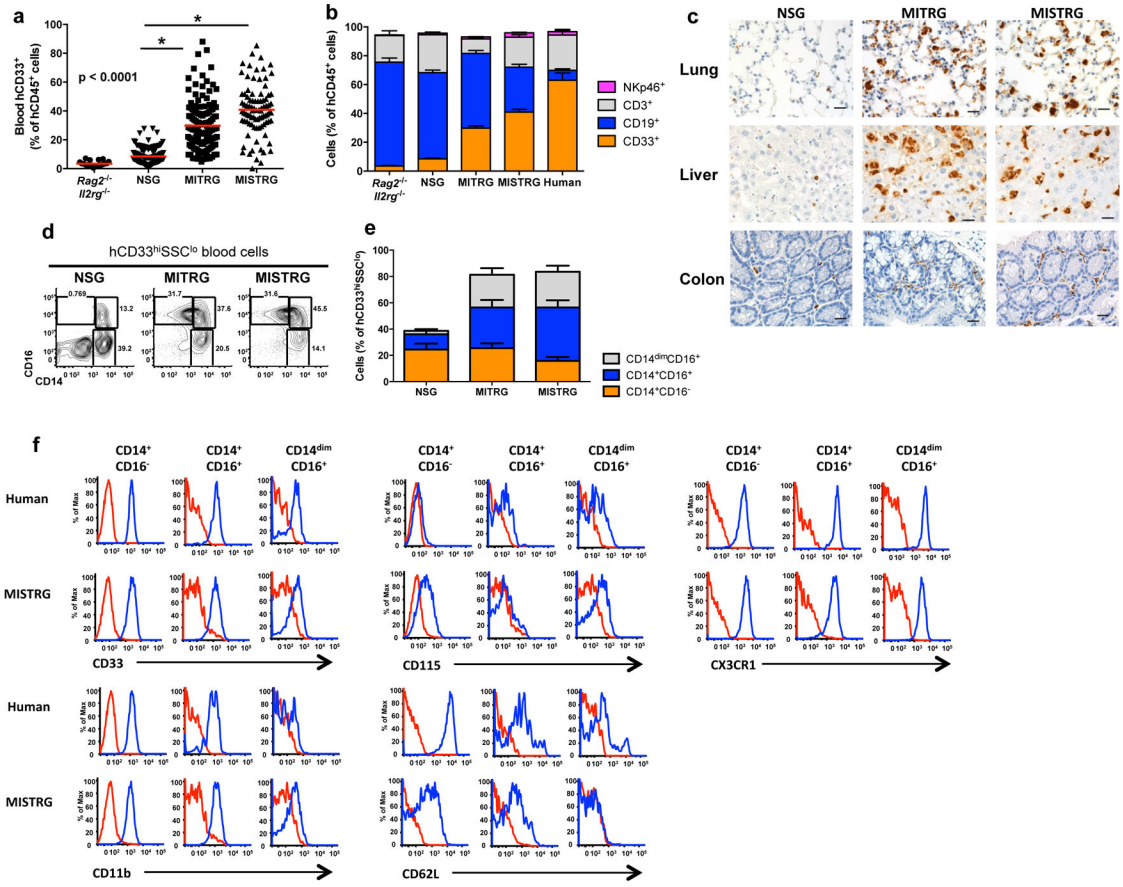

Fig. 2. MI(S)TRG mice support efficient myeloid cell development in lymphoid and non-lymphoid tissues

a, Percentages of human myeloid cells (hCD33$^+$) among human hematopoietic cells (hCD45$^+$) in the blood of the indicated recipient mice, engrafted as newborns by intra-hepatic injection of fetal liver CD34$^+$ cells after X-ray preconditioning. Each symbol represents an individual mouse and the red bars indicate mean values (n=20-113; statistical analysis is shown in Supplementary Fig. 3a). **b**, Composition of human white blood cells in the same mice as in **a** (n=20-113 mice/group; n=8 human donors; error bars indicate SEM). **c**, Immunohistological staining of human myeloid cells (hCD68$^+$) in non-lymphoid tissues of the indicated recipient mice. The black bar represents 20 μm, and the images shown are representative of at least three mice analyzed per group. **d-e**, Representative flow cytometry analysis (**d**) and frequencies (**e**) of human monocyte subsets, identified by expression of CD14 and CD16 among hCD45$^+$CD33$^+$ cells in the blood of recipient mice (n=8-12 mice/group; error bars indicate SEM). Dot plots in **d** are gated on CD33^{hi}SSC^{lo} cells to show the subset distribution among monocytic cells. **f**, Human monocytes in the blood of MISTRG recipients and human monocytes from a human donor were stained with the indicated antibodies. Staining with isotype control antibodies is shown in red and specific antibodies in blue.

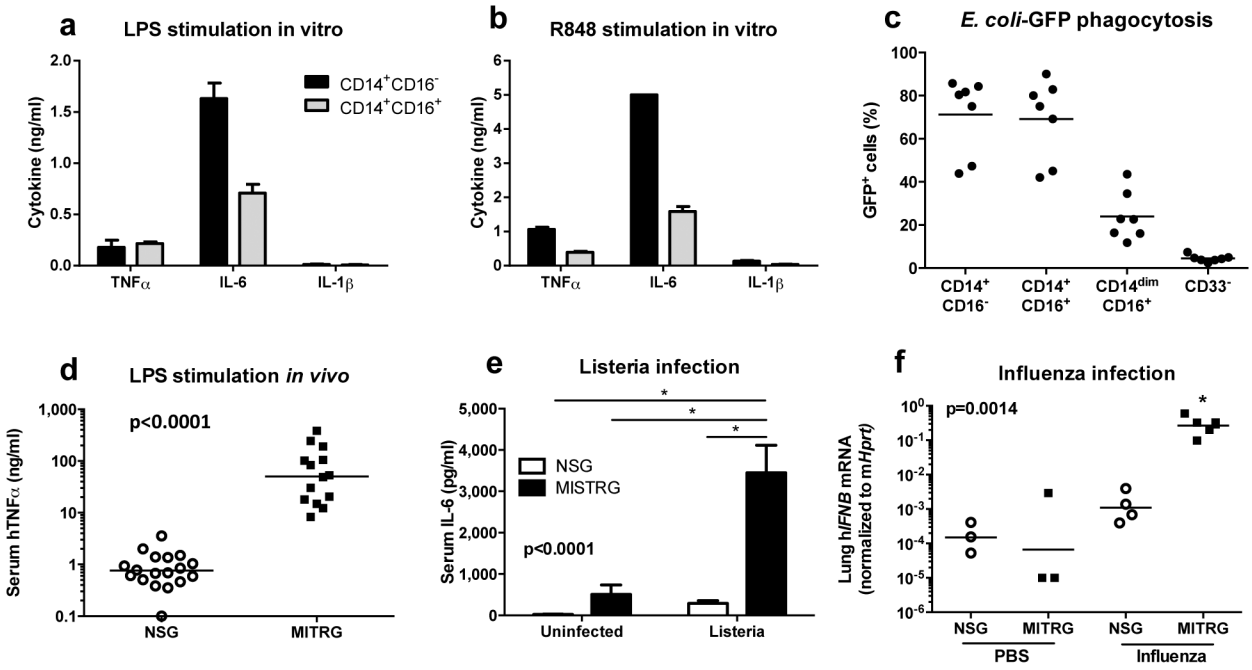

Fig. 3. Monocytes in MI(S)TRG mice are functional

a-b, Cytokine production by human monocytes isolated from the BM of MITRG recipients and stimulated overnight in vitro with 100 ng/ml LPS (**a**) or 10 μg/ml R848 (**b**) (error bars indicate SD of triplicates; representative of 3 independent experiments) was measured by ELISA. **c**, In vitro phagocytosis of GFP-expressing *E.coli* by human cell subsets, identified by flow cytometry gating, in the blood of MITRG mice (n=7). **d-f**, Mice were injected with LPS (**d**; 90 min, n=15-18), or infected with *Listeria monocytogenes* (**e**; day 2, n=6-15) or influenza A/PR8 H1N1 (**f**; day 3, n=3-5). Cytokine production was measured by ELISA (in the serum) or by RT-PCR (in the lung). (**d**) p-value calculated by unpaired Student's *t*-test on log10-transformed values; (**e,f**) p-values calculated by one-way ANOVA followed by Tukey posthoc test (* $p<0.05$).

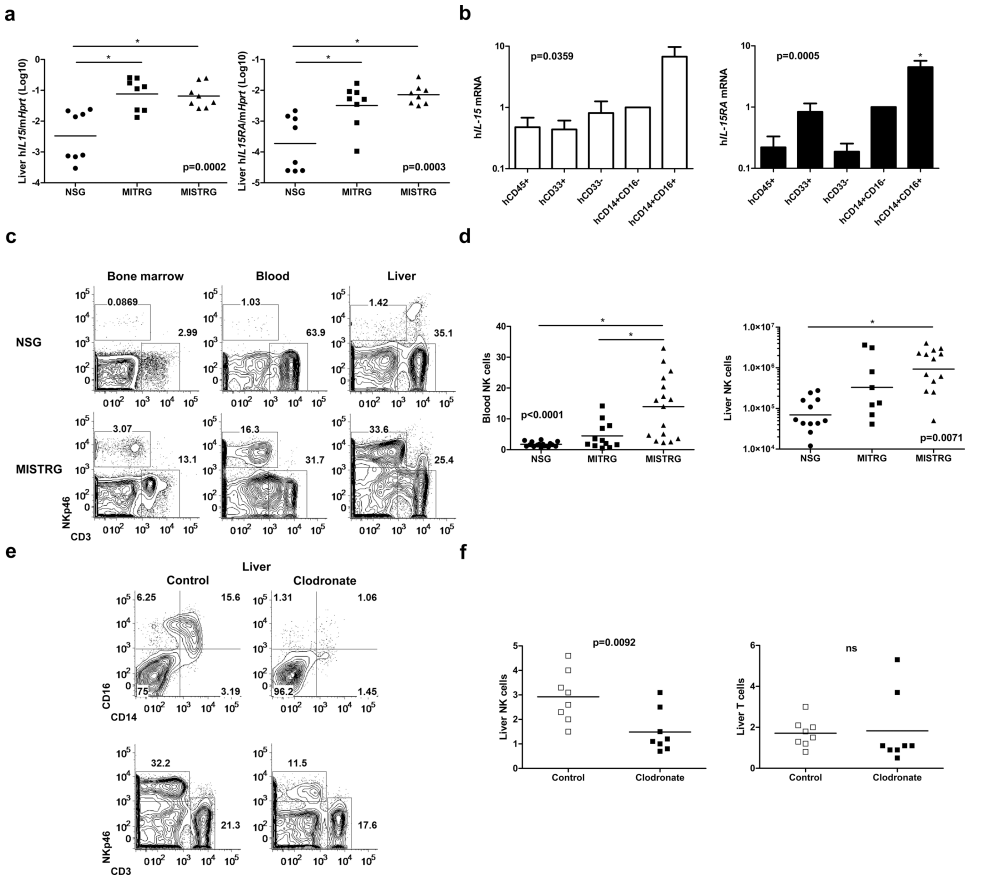

Fig. 4. Human NK cells develop efficiently in MISTRG mice

a, Quantitative RT-PCR analysis of human IL-15 and IL-15Rα mRNA expression in the liver of engrafted NSG, MITRG, and MISTRG mice (n=7-8; p-values calculated by one-way ANOVA; *, $p<0.05$ Tukey post hoc test). Expression was normalized to mouse *Hprt*. **b**, Quantitative RT-PCR analysis of human IL-15 and IL-15Rα mRNA expression in indicated human cell populations purified from bone marrow of engrafted MITRG mice (n=4-5, error bars indicate SEM). Expression was normalized to human *HPRT* and is shown relative to $hCD14^{+}hCD16^{-}$ cells. **c-d**, Representative flow cytometry analysis (gated on $hCD45^{+}mCD45^{-}$ cells, lymphocyte gate; numbers next to outlined areas indicate percentages of cells) (**c**) and absolute number or frequency (**d**) of human NK cells ($hNKp46^{+}$ $hCD3^{-}$) in engrafted NSG, MITRG, and MISTRG (n=8-16; p-values calculated by one-way ANOVA; *, $p<0.05$ Tukey post hoc test). **e-f**, Representative flow cytometry analysis (**e**) of human liver monocytes/macrophages (upper panel, gated on $hCD33^{+}$ cells) and NK cells, and absolute numbers (**f**) of human liver NK ($hNKp46^{+}hCD3^{-}$) and T cells ($hCD3^{+}$, shown as control) in engrafted MISTRG mice either left untreated or treated for 3 consecutive days with liposome-encapsulated clodronate to deplete phagocytic cells (n=8; p-value calculated by unpaired Student's *t*-test; ns, not significant). In **a,d,f**, each symbol represents an individual mouse. Black bars represent the mean. Results are combined from two (**a**, **e f**), three (**b**), or four (**c, d**) experiments.

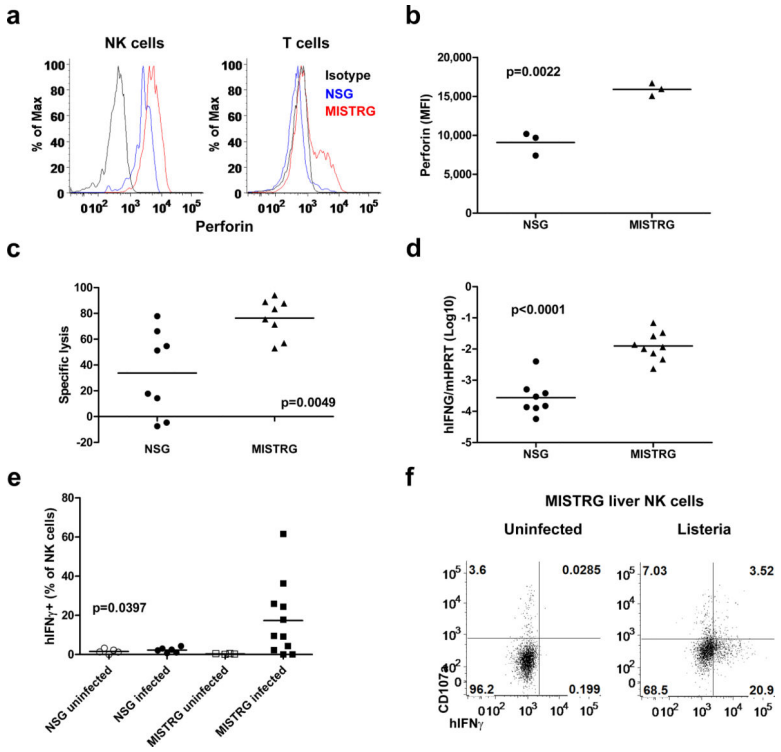

Fig. 5. Human NK cells in MITRSG mice are fully functional

a-b, Intracellular perforin expression by human liver NK (hNKp46^{+}hCD3^{-}) and T cells (hCD3^{+}) from engrafted NSG and MISTRG mice (n=3; p-value calculated by unpaired Student's *t*-test). MFI, mean fluorescence intensity. **c**, Violet-labeled LCL721.221 (HLA class I negative) and LCL721.45 (HLA class I positive) cells were injected i.v. in a 1:1 ratio, and the proportions of HLA class I positive or HLA class I negative cells among Violet-labeled cells recovered 12 hours later in the spleen, were used to calculate specific NK cell-mediated lysis (n=8, p-value calculated by unpaired student's t-test). **d**, Quantitative RT-PCR analysis of human IFN-γ mRNA expression in the liver of NSG and MISTRG mice 2 days after Listeria infection (n=8-9, p-value calculated by unpaired student's t-test). Expression was normalized to mouse *Hprt*. **e-f**, Frequency (**e**) and representative flow cytometry analysis (**f**) of IFN-γ-expressing and degranulating (CD107a^{+}) human liver NK cells from either uninfected or Listeria-infected NSG and MISTRG mice (n=4-11; p-value calculated by one-way ANOVA). In (**b-e**), each symbol represents an individual mouse. Black bars represent the mean. Results are representative of or combined from two experiments.

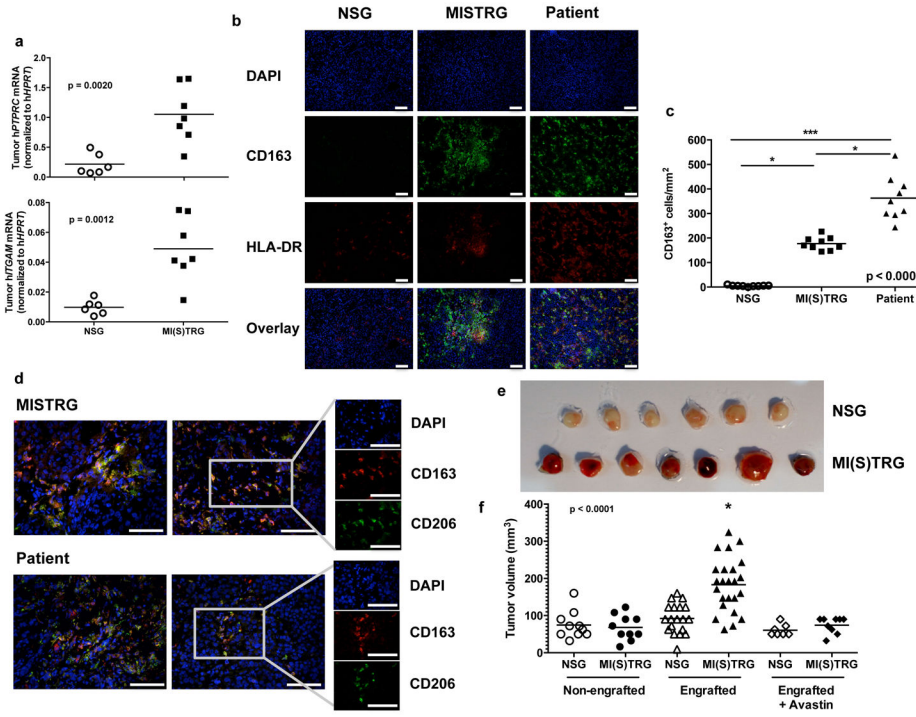

Fig. 6. Infiltration and growth of a tumor in MISTRG mice

The human melanoma cell line Me290 was subcutaneously implanted in the flank of engrafted or non-engrafted NSG and MI(S)TRG mice. Where indicated mice were treated with the VEGF-inhibitor Avastin™ every two days, starting on the day of tumor injection. The tumors were measured and dissected for analysis 11 days later. **a**, Inflitration of human hematopoietic cells in the tumor, determined by the expression of *PTPRC* mRNA (encoding CD45) and *ITGAM* mRNA (encoding CD11b) (n=6-7; p-value calculated by unpaired Sudent's t-test). **b** and **d**, Representative immunohistochemistry images of human myeloid cell markers in tumors from NSG, MISTRG and human patients (the white scale bars indicate 100 μm). **c**, Quantification of the density of $CD163^+$ cells in tumors (n=3 samples/group, 3 slides counted/sample). **e-f**, Representative pictures (**e**) and volume (**f**) of the tumors in the indicated groups of mice (n=7-24 mice/group). p-values were calculated by Student's *t*-test (**a**) or by one-way ANOVA (**c, e**) followed by Tukey posthoc test (* p<0.05).